Inorg. Chem. **2004**, *43*, 8290–8300

Paramagnetic Precursors for Supramolecular Assemblies: Selective Syntheses, Crystal Structures, and Electrochemical and Magnetic Properties of $Ru_2(O_2CMe)_{4-n}$(formamidinate)$_n$Cl Complexes, $n = 1$–4

Panagiotis Angaridis, F. Albert Cotton,* Carlos A. Murillo,* Dino Villagrán, and Xiaoping Wang

Department of Chemistry and Laboratory for Molecular Structure and Bonding, P.O. Box 30012, Texas A&M University, College Station, Texas 77842-3012

Received July 7, 2004

Reactions of $Ru_2(O_2CMe)_4Cl$ with two formamidines, HDXyl^{2,6}F = *N*,*N*′-di(2,6-xylyl)formamidine and HDAniF = *N*,*N*′-di(*p*-anisyl)formamidine, have been investigated with the idea of synthesizing compounds with a mixed set of ligands having different labilities to be used as precursors of paramagnetic, higher-order assemblies. Depending on the formamidine and the reaction conditions, several Ru_2^{5+} compounds of the type $Ru_2(O_2CMe)_{4-n}(DArF)_nCl$ (DArF = anion of an *N*,*N*′-diarylformamidine) have been isolated. With the bulky formamidine HXyl^{2,6}F, the compounds $Ru_2(O_2CMe)_3(DXyl^{2,6}F)Cl$ (**1**) and *trans*-$Ru_2(O_2CMe)_2(DXyl^{2,6}F)_2Cl$ (**2**) were obtained. From reactions with appropriate amounts of HDAniF in THF and in the presence of NEt_3 and LiCl, complexes of the general type $Ru_2(O_2CMe)_{4-n}(DArF)_nCl$ ($n = 1$–4) were selectively obtained. For $n = 2$, only the cis isomer was obtained. The choice of solvent in reactions of $Ru_2(O_2CMe)_4Cl$ and HDAniF is of great importance. Toluene favored the formation of the fully substituted Ru_2^{5+} complex $Ru_2(DAniF)_4Cl$ (**3**), whereas MeOH resulted in a disproportionation reaction that gave the edge-sharing bioctahedral $Ru^{3+}Ru^{3+}$ complex [*trans*-$Ru_2(\mu\text{-}OMe)_2(\mu\text{-}O_2CMe)_2(HDAniF)_4]Cl_2$ (**6**) and the Ru_2^{4+} complex $Ru_2(DAniF)_4$ (**7**). Complexes **6** and **7** with an Ru_2^{6+} and Ru_2^{4+} core, respectively, are diamagnetic, whereas all Ru_2^{5+} complexes are paramagnetic with $\sigma^2\pi^4\delta^2(\pi^*\delta^*)^3$ ground-state electronic configurations and large zero-field splitting contributions. All compounds show rich and complex electrochemical behavior.

Introduction

There is currently great interest in the study of supramolecular assemblies containing metal atom centers as building blocks.[1] Much work has been done using single atom centers, but recent pioneering work has been done in the use of building blocks with metal−metal bonded units, e.g., those derived from quadruply bonded Mo_2^{4+} units or those having singly bonded Rh_2^{4+} units that can be linked by a variety of dianions such as dicarboxylates, diamidates, and oxoanions such as those of the type MO_4^{2-}, M = S, Mo, and W.[2] Units of this type allow a variety of architectures, and these compounds are characterized by being diamagnetic and having rich electrochemistry, which has been used to probe electronic communication. An important advantage offered by the use of M−M bonded corner pieces is that a wide selection of transition metal atoms can be employed. These exhibit a variety of electronic configurations that are generally well understood.[3] However, a necessary prerequisite to further systematic studies is the design and selective synthesis of appropriate dimetal precursors containing mixed sets of labile and nonlabile ligands. Precursors with a *cisoid* arrangement of two nonlabile groups react with rigid dianions to form squares or, in some circumstances, triangles. With inherently bent linkers, loops can be formed.[2] Conversely,

* To whom correspondence should be addressed. E-mail: cotton@tamu.edu (F.A.C.), murillo@tamu.edu (C.A.M.).

(1) See, for example: (a) Fujita, M. *Acc. Chem. Res*. **1999**, *32*, 53. (b) Lehn, J.-M. *Supramolecular Chemistry—Concepts and Perspectives*; VCH: Weinheim, Germany, 1995. (c) Kim, J.; Chen, B.; Reineke, T. M.; Li, H.; Eddaoudi, M.; Moler, D. B.; O'Keeffe, M.; Yaghi, O. M. *J. Am. Chem. Soc*. **2001**, *123*, 8239. (d) Fujita, M. *Chem. Soc. Rev*. **1998**, *27*, 417. (e) Leininger, S.; Olenyuk, B.; Stang, P. J. *Chem. Rev*. **2000**, *100*, 853. (f) Holliday, G. J.; Mirkin, C. A. *Angew. Chem., Int. Ed*. **2001**, *40*, 2022. (g) Swieger, G. F.; Malefetse, T. J. *Chem. Rev*. **2000**, *100*, 3483. (h) Navarrro, J. A. R.; Lippert, B. *Coord. Chem. Rev*. **1999**, 915.

(2) See, for example: (a) Cotton, F. A.; Lin, C.; Murillo, C. A. *Acc. Chem. Res*. **2001**, *34*, 759. (b) Cotton, F. A.; Liu, C. Y.; Murillo, C. A.; Villagrán, D.; Wang, X. *J. Am. Chem. Soc*. **2003**, *125*, 13564. (c) Cayton, R. H.; Chisholm, M. H.; Huffman, J. C.; Lobkovsky, E. B. *J. Am. Chem. Soc.* **1991**, *113*, 8709.

(3) Cotton, F. A.; Walton, R. A. *Multiple Bonds between Metal Atoms*, 2nd ed.; Oxford University Press: Oxford, U.K., 1993.

10.1021/ic049108w CCC: $27.50
Published on Web 11/20/2004

precursors with a *transoid* arrangement of nonlabile groups could be expected to form ladder structures. Precursors with three formamidinate groups in equatorial positions form pairs that, upon one-electron oxidations, produce mixed-valence compounds that resemble the Creutz−Taube ion.[4] More complex architectures could be expected from a precursor with only one nonlabile bridging group. Recent work with dimolybdenum units has shown that a series of complexes with mixed-ligand sets of different labilities can be prepared. Selective substitution of the labile ligands allows the synthesis of various types of supramolecular products containing Mo_2 units.[5]

An appealing group of compounds that could be used as subunits in supramolecular assemblies are those having a diruthenium core, not only because Ru_2^{n+} cores show rich redox chemistry but also because they provide magnetic properties for further study. Dinuclear ruthenium complexes have been isolated in three different oxidation states (Ru_2^{4+}, Ru_2^{5+}, and Ru_2^{6+}),[6] and they usually adopt a paddlewheel structure, although sometimes compounds with face-sharing bioctahedral structures are found. In the former structural type, four uninegative, three-atom ligands span pairs of multiply bonded Ru atoms. The type of bridging ligand affects not only the geometrical characteristics but also the electronic structures, which in turn have a profound effect on the magnetic properties, as shown in diruthenium complexes with *N*,*N*′- and *O*,*O*′-donor bridging ligands.[3] For example, the diruthenium complex $Ru_2(O_2CMe)_4(THF)_2$, with four *O*,*O*′-donor bridging ligands, exhibits a short Ru−Ru distance of 2.261(3) Å and is paramagnetic with a $\sigma^2\pi^4\delta^2\delta^{*2}\pi^{*2}$ electronic configuration.[7] In contrast, the analogous complex $Ru_2(DTolF)_4$, with four *N*,*N*′-di(*p*-tolyl)-formamidinate (DTolF) bridging ligands, is diamagnetic with a $\sigma^2\pi^4\delta^2\pi^{*4}$ ground-state electronic configuration and has a long Ru−Ru distance of 2.474(1) Å.[8] In the latter complex, it is the interaction of the frontier orbitals of the Ru_2^{4+} core with the orbitals of the basic bridging ligands, resulting in the elevation of the δ^* molecular orbital above the π^* molecular orbital, that gives the closed-shell electronic configuration.[8] In contrast, the Ru_2^{5+} complex $Ru_2(DTolF)_4Cl$ is paramagnetic with a $\sigma^2\pi^4\delta^2(\pi^*\delta^*)^3$ electronic configuration and has a Ru−Ru bond distance of 2.370(2) Å.[9] Here, the π^* and δ^* molecular orbitals are almost degenerate. Furthermore, there have been reports of complexes with a Ru_2^{5+} core and four *N*,*N*′-donor bridging ligands that exhibit an $S = {}^1/_2$ state, an example being $[Ru_2(DTolTA)_4(MeCN)](BF_4)$ [DTolTA = di(*p*-tolyl)triazenate].[10] This was attributed to the effect of the high basicity of the DTolTA ligand, which pushes the energy of the δ^* orbitals above that of the π^* orbitals.[8] As a result, the $\sigma^2\pi^4\delta^2\pi^{*3}$ ground-state electronic configuration was proposed.

Recently, we reported the synthesis and magnetic properties of two diruthenium complexes with mixed sets of acetate/formamidinate bridging ligands *cis*-$Ru_2(O_2CMe)_2(DAniF)_2Cl$[11] and $Ru_2(O_2CMe)(DAniF)_3Cl$ [DAniF = *N*,*N*′-di(*p*-anisyl)-formamidinate, (*p*-MeO−$C_6H_4N)_2CH$].[12] Both are paramagnetic with $S = {}^3/_2$ and have been used as precursors of the first paramagnetic supramolecular assemblies based on diruthenium end or corner pieces. To extend our quest for other potential diruthenium building blocks while keeping in mind the unusual magnetic properties of diruthenium complexes, efforts have been made to synthesize selectively the complete series of complexes with formulas $Ru_2(O_2CMe)_{4-n}(DArF)_nCl$ (**I**−**V**), where $n = 1$, 2 (cis and trans), 3, 4 and Ar = an aryl group, and to study their magnetic properties.

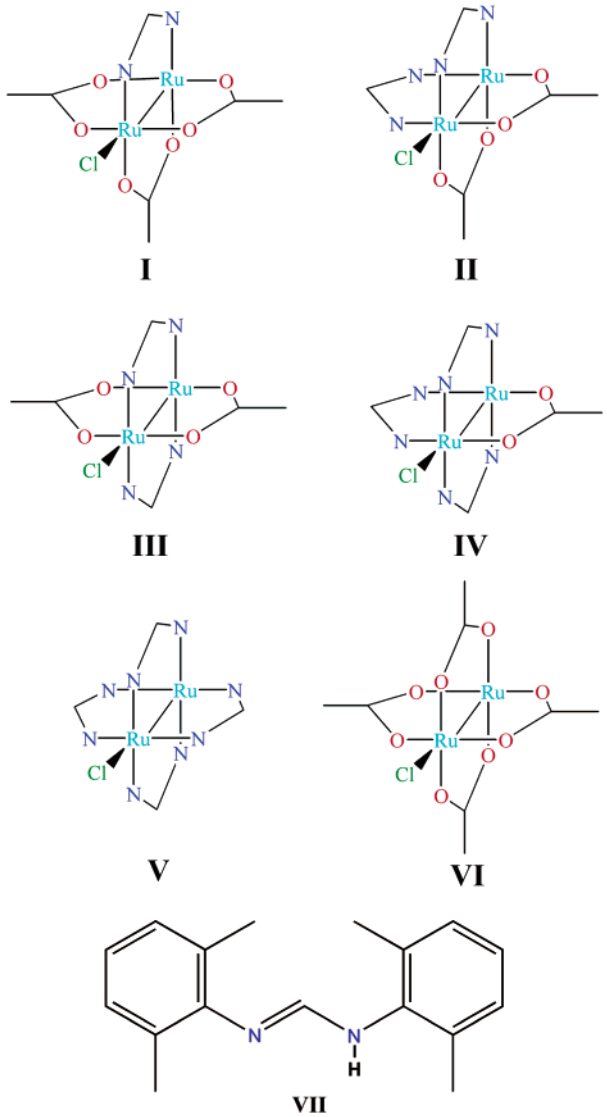

In this report, we describe the syntheses, structural characterizations, and electrochemical and magnetic proper-

(4) Cotton, F. A.; Liu, C. Y.; Murillo, C. A.; Villagrán, D.; Wang, X. *J. Am. Chem. Soc.* **2004**, *126*, 14822.
(5) Cotton, F. A.; Liu, C. Y.; Murillo, C. A. *Inorg. Chem.* **2004**, *43*, 2267.
(6) Aquino, M. A. S. *Coord. Chem. Rev.* **1998**, *170*, 141.
(7) Lindsay, A. J.; Wilkinson, G.; Motevalli, M.; Hursthouse, M. B. *J. Chem. Soc., Dalton Trans.* **1985**, 2321.
(8) Cotton, F. A.; Ren, T. *Inorg. Chem.* **1991**, *30*, 3675.
(9) Cotton, F. A.; Ren, T. *Inorg. Chem.* **1995**, *34*, 3190.
(10) Cotton, F. A.; Falvello, L. R.; Ren, T.; Vidyasagar, K. *Inorg. Chim. Acta* **1992**, *194*, 163.
(11) Angaridis, P.; Berry, J. F.; Cotton, F. A.; Murillo, C. A.; Wang, X. *J. Am. Chem. Soc.* **2003**, *125*, 10327.
(12) Angaridis, P.; Berry, J. F.; Cotton, F. A.; Lei, P.; Lin, C.; Murillo, C. A.; Villagrán, D. *Inorg. Chem. Commun.* **2004**, *7*, 9.

ties of Ru_2^{5+} complexes with mixed sets of bridging formamidinate and acetate ligands isolated from reactions of $Ru_2(O_2CMe)_4Cl$, **VI**, with two formamidines that have significantly different steric requirements, *N*,*N*′-2,6- dixylylformamidine ($HDXyl^{2,6}F$, **VII**) and HDAniF. In this way, a variety of compounds, including cis and trans isomers of $Ru_2(O_2CMe)_2(formamidinate)_2Cl$ compounds, can be selectively prepared. An improved synthesis for the cis complex with DAniF is also provided. An extensive discussion of the effects of the experimental conditions (temperature, solvent, nature of the formamidinate, reaction time, and ratio of the reactants) on these reactions is an important part of this account. The new or improved syntheses reported here are for the compounds $Ru_2(O_2CMe)_3(DXyl^{2,6}F)Cl(THF)$ (**1a**), $Ru_2(O_2CMe)_3(DXyl^{2,6}F)Cl(HDXyl^{2,6}F)$ (**1b**), *trans*-$Ru_2(O_2CMe)_2(DXyl^{2,6}F)_2Cl(THF)$ (**2a**), *trans*-$Ru_2(O_2CMe)_2(DXyl^{2,6}F)_2Cl$ (**2b**), $Ru_2(O_2CMe)_3(DAniF)Cl$ (**3**), *cis*-$Ru_2(O_2CMe)_2(DAniF)_2Cl$ (**4**), $Ru_2(DAniF)_4Cl$ (**5**), [*trans*-$Ru_2(\mu\text{-}OMe)_2(\mu\text{-}O_2CMe)_2(HDAniF)_4]Cl_2$ (**6**), and $Ru_2(DAniF)_4$ (**7**). Crystal structures are provided for **1a**, **1b**, **2a**, **2b**, **5**, **6**, and **7**.

Experimental Section

Materials and Methods. All reactions and manipulations were performed under a nitrogen atmosphere, using standard Schlenk line techniques. Commercial-grade solvents were dried over appropriate drying agents and deoxygenated by reflux for at least 24 h under a N_2 atmosphere. They were freshly distilled prior to use. The diruthenium starting material $Ru_2(O_2CMe)_4Cl$ was prepared as described in the literature.[13] The formamidines $HDXyl^{2,6}F$ and HDAniF were prepared according to a published general procedure.[14]

Mass spectrometry data (electrospray ionization) were recorded at the Laboratory for Biological Mass Spectrometry at Texas A&M University, using an MDS Series Qstar Pulsar with a spray voltage of 5 kV. Elemental analyses were performed by Canadian Microanalytical Service, Ltd., Delta, British Columbia, Canada. Infrared spectra were recorded with a Perkin-Elmer 16PC FT IR spectrophotometer as KBr pellets. ^1H NMR spectra were recorded on a Mercury 300 NMR spectrometer. Cyclic voltammograms were collected on a CH Instruments model CH1620A electrochemical analyzer, with Pt working and auxiliary electrodes and a Ag/AgCl reference electrode. The scan rate was 0.10 V/s. The $E_{1/2}$ values were obtained from the relationship $E_{1/2} = (E_{ap} + E_{cp})/2$. The experiments were performed at room temperature under a nitrogen atmosphere in THF solutions that contained 0.1 M $(Bu^n_4N)PF_6$ as the supporting electrolyte. All the potentials were referenced to the Ag/AgCl electrode, and under our experimental conditions, $E_{1/2}$ for the Fc/Fc^+ couple occurred at +0.600 V. Variable-temperature magnetic susceptibility measurements were obtained with a Quantum Design SQUID Magnetometer MPMS-XL at 1000 G, and the data were corrected for diamagnetism.

Synthesis of $Ru_2(O_2CMe)_3(DXyl^{2,6}F)Cl$ (1). To a mixture of $Ru_2(O_2CMe)_4Cl$ (0.105 g, 0.220 mmol) and $HDXyl^{2,6}F$ (0.551 g, 2.18 mmol) was added 15 mL of toluene. The brown suspension was stirred and refluxed for 36 h, resulting in a red mixture, which was filtered to remove a small amount of unreacted $Ru_2(O_2CMe)_4Cl$. About 50 mL of hexanes was added to the filtrate under stirring, resulting in the precipitation of a red solid. After removal of the supernatant liquid, the solid was washed with a 1:1 mixture of hexanes and Et_2O (40 mL) and dried under vacuum. Addition of THF (10 mL) to the solid resulted in a red solution that was layered with 30 mL of hexanes. Brown-red crystals of $Ru_2(O_2CMe)_3(DXyl^{2,6}F)Cl(THF)\cdot 0.5THF$ (**1a**·0.5THF) were grown over a period of 2−3 days. Yield: 0.047 g (32%). Anal. Calcd (found): C 41.47 (41.78), H 4.21 (4.29), N 4.21 (4.09)%. +ESI-MS (CH_2Cl_2, *m*/*z*): 631 ($[M - Cl]^+$). IR (KBr disk, cm^{-1}): 3449 w, 3198 w, 3126 w, 2959 w, 2366 w, 1627 w, 1502 s, 1441 s, 1351 sh, 1294 m, 1200 m, 1097 m, 1034 m, 771 m, 689 s, 625 w. CV (V vs Ag/AgCl): $E_{ap}(1) = +1.295$ V, $E_{1/2}(2) = -0.185$ V [$E_{ap}(2) = -0.142$ V and $E_{cp}(2) = -0.228$ V], $E_{cp}(3) = -0.627$ V. Crystals of $Ru_2(O_2CMe)_3(DXyl^{2,6}F)Cl(HDXyl^{2,6}F)\cdot$toluene (**1b**·toluene) were grown by dissolving the crude product (before the recrystallization in THF) in toluene and adding a layer of hexanes.

Synthesis of *trans*-$Ru_2(O_2CMe)_2(DXyl^{2,6}F)_2Cl$ (2). A mixture of $Ru_2(O_2CMe)_4Cl$ (0.100 g, 0.210 mmol) and $HDXyl^{2,6}F$ (0.517 g, 2.05 mmol) was heated at ∼150 °C for 5 h. During that time, the molten mixture turned dark red. After removal of the excess of $HDXyl^{2,6}F$ by vacuum sublimation at ∼130 °C, the dark solid was extracted with 10 mL of toluene. To the red filtrate was added a portion of about 40 mL of hexanes. The red mixture was stirred for 30 min, resulting in the precipitation of a red microcrystalline solid, which was collected by filtration. This solid was dried under vacuum and then dissolved in 15 mL of THF, and the solution was layered with 30 mL of hexanes. Red crystals of *trans*-$Ru_2(O_2CMe)_2(DXyl^{2,6}F)_2Cl(THF)$ (**2a**) were obtained in a few days. Yield: 0.128 g (71%). Anal. Calcd (found): C 53.18 (53.56), H 5.13 (5.21), N 6.53 (6.41)%. +ESI-MS (CH_2Cl_2, *m*/*z*): 824 ($[M - Cl]^+$). IR (KBr disk, cm^{-1}): 2955 w, 1528 s, 1465 m, 1439 s, 1318 m, 1254 w, 1318 m, 1194 s, 1095 m, 1040 m, 887 m, 774 m, 686 m, 455 m. CV (V vs Ag/AgCl): $E_{1/2}(1) = +0.933$ V [$E_{ap}(1) = +0.978$ V and $E_{cp}(1) = 0.888$ V], $E_{1/2}(2) = -0.358$ V [$E_{ap}(2) = -0.303$ V and $E_{cp}(2) = -0.412$ V], $E_{cp}(3) = -0.830$ V. Crystals of *trans*-$Ru_2(O_2CMe)_2(DXyl^{2,6}F)_2Cl\cdot 2$toluene (**2b**·2toluene) were grown by dissolving the crude product in toluene (instead of carrying out the dissolution in THF) and adding a layer of hexanes.

Synthesis of $Ru_2(O_2CMe)_3(DAniF)Cl$ (3). To a suspension of $Ru_2(O_2CMe)_4Cl$ (0.156 g, 0.330 mmol) in 20 mL of THF was added HDAniF (0.128 g, 0.500 mmol). The mixture was stirred and heated gently (at a temperature not higher than 45 °C) for 12 h, resulting in a color change to dark purple. After filtration of a small amount of unreacted $Ru_2(O_2CMe)_4Cl$, the solvent from the filtrate was removed under vacuum to leave a dark residue. This solid was dissolved in 4−5 mL of MeCN, and the resulting solution was passed through a chromatographic column [silica gel; eluent (v/v) $THF/CH_2Cl_2 = 5:1$]. Three bands eluted. The first one was slightly tinted (violet-purple) and contained unreacted HDAniF. This was followed by a purple-red band containing the product and then a green band containing *cis*-$Ru_2(O_2CMe)_2(DAniF)_2Cl$. The purple-red band was collected, and after evaporation of the solvent, a purple-red solid was isolated. Yield: 0.062 g (28%). Anal. Calcd (found): C 37.65 (37.58), H 3.61 (3.82), N 4.18 (4.06)%. +ESI-MS (CH_2Cl_2, *m*/*z*): 634 ($[M - Cl]^+$). IR (KBr disk, cm^{-1}): 3333 w, 2953 w, 2835 w, 1645 m, 1599 sh, 1503 s, 1440 s, 1292 m, 1246 s, 1179 sh, 1109 w, 1030 m, 835 m, 690 m. CV (V vs Ag/AgCl in CH_2Cl_2): $E_{1/2}(1) = 1.61$ V [$E_{ap}(1) = +1.57$ V and $E_{cp}(1) = 1.64$ V], $E_{1/2}(2) = 1.13$ V [$E_{ap}(2) = 1.03$ V and $E_{cp}(2) = 1.23$ V].

Synthesis of *cis*-$Ru_2(O_2CMe)_2(DAniF)_2Cl$ (4). To a mixture of $Ru_2(O_2CCH_3)_4Cl$ (0.237 g, 0.500 mmol), HDAniF (0.256 g, 1.00 mmol), NEt_3 (1.5 mg, 1.5 mmol), and LiCl (0.50 g) was added

(13) (a) Stephenson, T. A.; Wilkinson, G. *J. Inorg. Nucl. Chem.* **1966**, *28*, 2285. (b) Mitchell, R. W.; Spencer, A.; Wilkinson, G. *J. Chem. Soc., Dalton Trans.* **1973**, 846.

(14) Roberts, R. M. *J. Org. Chem.* **1949**, *14*, 277.

THF (30 mL). The red mixture was heated to reflux for 18 h. The color changed gradually to very dark green. After the volatile materials had been removed under vacuum, benzene (2 × 15 mL) was added to the solid, and the mixture filtered through a frit packed with Celite. The volume of the solution was reduced to ca. 10 mL, and then hexanes (50 mL) was added under stirring to produce a solid. This solid was collected by filtration and dissolved in a minimum amount of benzene, and a layer of hexanes (60 mL) was then added. After 2 days, large dark green crystals of *cis*-$Ru_2(O_2CMe)_2(DAniF)_2Cl$ were obtained. Yield: 0.367 g (85%). Cyclic voltammetry data, in THF using $(Bu^n_4N)PF_6$ as the electrolyte (V vs Ag/AgCl): $E_{1/2}(1) = +0.817$ V [$E_{ap}(1) = +0.866$ V and $E_{cp}(1) = +0.768$ V], $E_{ap}(2) = -0.297$ V, $E_{cp}(3) = -0.668$ V, $E_{cp}(4) = -1.528$ V.

Synthesis of $Ru_2(DAniF)_4Cl$ (5). To a mixture of $Ru_2(O_2CMe)_4Cl$ (0.097 g, 0.200 mmol) and HDAniF (0.551 g, 2.15 mmol) was added 15 mL of toluene. The suspension was stirred and refluxed for 48 h, resulting in a very dark mixture. After the solid had been allowed to settle, the supernatant liquid was removed using a cannula. The microcrystalline solid left in the flask was washed with toluene (2 × 20 mL) and dried under vacuum. This was then dissolved in 20 mL of CH_2Cl_2, giving a dark green solution that was layered with 30 mL of hexanes. Dark green-purplish crystals of $Ru_2(DAniF)_4Cl\cdot 0.5CH_2Cl_2$ (**5**·$0.5CH_2Cl_2$) grew over a period of 3−4 days. Yield: 0.206 g (84%). Anal. Calcd (found): C 57.21 (57.04), H 4.77 (4.69), N 8.89 (8.95)%. +ESI-MS (CH_2Cl_2, *m*/*z*): 1224 ($[M - Cl]^+$). IR (KBr disk, cm^{-1}): 3447 w, 2957 w, 2828 w, 2368 w, 1603 m, 1547 m, 1503 vs, 1457 m, 1337 m, 1291 m, 1243 s, 1214 s, 1172 m, 1106 m, 1031 s, 930 w, 827 m, 830 sh, 588 w. CV (V vs Ag/AgCl): $E_{1/2}(1) = +0.431$ V [$E_{ap}(1) = +0.480$ V and $E_{cp}(1) = +0.382$ V], $E_{ap}(2) = -0.155$ V, $E_{cp}(3) = -0.754$ V, $E_{1/2}(4) = -1.662$ V [$E_{ap}(4) = -1.609$ V and $E_{cp}(4) = -1.716$ V].

Syntheses of [*trans*-$Ru_2(\mu\text{-}OMe)_2(\mu\text{-}O_2CMe)_2(HDAniF)_4]Cl_2$ (6) and $Ru_2(DAniF)_4$ (7). To a mixture of $Ru_2(O_2CMe)_4Cl$ (0.240 g, 0.500 mmol) and HDAniF (0.545 g, 2.10 mmol) was added 30 mL of MeOH. The mixture was stirred and refluxed for 15 h, resulting in a dark green-brown solution phase and a red microcrystalline precipitate. After filtration, the crystalline precipitate was saved (see below), and the filtrate was evaporated to dryness to leave a dark solid in the flask. After the solid had been dried under vacuum, it was dissolved in 10 mL of toluene and precipitated by addition of 30 mL of hexanes. This solid was washed with hexanes (2 × 30 mL) and then dissolved in 10 mL of CH_2Cl_2. Addition of 40 mL of Et_2O resulted in the precipitation of an orange solid that was collected and dried under vacuum. This solid was dissolved in 15 mL of CH_2Cl_2, and the resulting solution was layered with 35 mL of Et_2O. Orange crystals of [*trans*-$Ru_2(\mu\text{-}OMe)_2(\mu\text{-}O_2CMe)_2(HDAniF)_4]Cl_2\cdot 4MeOH$ (**6**·4MeOH) were obtained after a few days. Yield: 0.187 g (25% based on total Ru). Anal. Calcd (found): C 53.62 (53.38), H 5.14 (5.19), N 7.58 (7.43)%. +ESI-MS (CH_2Cl_2, *m*/*z*): 1407 ($[M - 2Cl]^+$), 1151 ($[M - 2Cl - HDAniF]^+$). ^{1}H NMR δ (ppm, $CDCl_3$): 1.96 (s, 6H, $-O_2CCH_3$), 3.68 [s, 6H, $-OCH_3$-(bridging)], 3.84 (s, 24H, $-OCH_3$), 6.78 (d, 16H, aromatic), 6.92 (d, 16H, aromatic), 8.73 (s, 4H, $-NCHN-$), 11.93 (broad, 4H, $-NH-$). IR (KBr disk, cm^{-1}): 3377 m, 3200 sh, 2962 m, 2959 sh, 2833 m, 1631 vs, 1592 sh, 1552 m, 1507 vs, 1439 s, 1409 s, 1295 s, 1248 vs, 1177 s, 1106 s, 1025 s, 827 m, 752 w, 722 w, 608 w, 538 m, 473 w. The red microcrystalline solid, isolated from the reaction mixture, was washed with MeOH and dried under vacuum. It was then dissolved in 20 mL of toluene, and the resulting solution was layered with hexanes. Dark red crystals of $Ru_2(DAniF)_4(H_2O)_{0.5}$ (**7**) were obtained over a period of 1 week. Yield: 0.148 g (24% based on total Ru). ^{1}H NMR δ (ppm, benzene-d^6): 3.74 (s, 24H, $-OCH_3$), 6.68 (d, 16H, aromatic), 7.01 (d, 16H, aromatic), 9.28 (s, 4H, $-NCHN-$).

X-ray Crystallography. Crystals of **1a**·0.5THF, **1b**·toluene, **2a**, **2b**·2toluene, **5**·$0.5CH_2Cl_2$, **6**·4MeOH, and **7** were mounted on the end of quartz fibers and used for intensity data collection on a Bruker SMART 1000 CCD area detector system equipped with a liquid nitrogen low-temperature controller using Mo Kα radiation. Cell parameters were obtained using SMART software.[15] Data reduction and integration were performed using the software package SAINT PLUS,[16] which also corrects for Lorentz and polarization effects, while absorption corrections were applied using the program SADABS.[17] In all structures, the positions of heavy atoms were found via direct methods using the SHELXTL software.[18] Subsequent cycles of least-squares refinement followed by difference Fourier syntheses revealed the positions of the remaining non-hydrogen atoms. All non-hydrogen atoms were refined anisotropically, except for the disordered THF molecule in **1a**·0.5THF, the aryl groups in **1b**·toluene and **2a**, the toluene molecules in **2b**·2toluene, the dichloromethane molecule in **5**·$0.5CH_2Cl_2$, the methanol molecule, and the Cl^- ions in **6**·4MeOH. Hydrogen atoms were placed at calculated idealized positions. Cell parameters and basic information pertaining to data collection and structure refinement for compounds **1a**, **1b**, **2a**, **2b**, **5**, **6**, and **7** are summarized in Table 1.

Results and Discussion

It has been known since 1995 that Ru_2^{5+} tetraformamidinate compounds can be synthesized from the reactions of $Ru_2(O_2CMe)_4Cl$ with molten neutral formamidines at elevated temperatures (>150 °C).[9] More recently, an alternative method was reported in a brief communication by Ren and co-workers according to which a mixture of $Ru_2(O_2CMe)_4Cl$ with an excess of a formamidine is heated to reflux in THF in the presence of NEt_3 and excess LiCl.[19] Given our interest in the synthesis of Ru_2^{5+} complexes with mixed sets of bridging, nonlabile formamidinate and labile acetate ligands as suitable precursors for the construction of supramolecular assemblies, our efforts focused on the study of similar reactions, but carried out under mild conditions. We have succeeded in selectively synthesizing all complexes of the general type $Ru_2(O_2CMe)_{4-n}(DArF)_nCl$ ($n = 1-4$) by using two different formamidines: $HDXyl^{2,6}F$ and HDAniF.

Reactions with $HDXyl^{2,6}F$. Two complexes were isolated from the reactions of $Ru_2(O_2CMe)_4Cl$ with $HDXyl^{2,6}F$ (Scheme 1). In refluxing toluene (ca. 110 °C) and in the presence of a 10-fold excess of $HDXyl^{2,6}F$, only one acetate group was replaced, resulting in the mono-formamidinate complex $Ru_2(O_2CMe)_3(DXyl^{2,6}F)Cl$ (**1**). At temperatures <100 °C, acetate substitution does not take place. However, at higher temperatures (∼160 °C) and when molten $HDXyl^{2,6}F$

(15) *SMART. Data Collection Software*, version 5.618; Bruker Advanced X-ray Solutions, Inc.: Madison, WI, 2000.
(16) *SAINTPLUS. Data Reduction Software*, version 6.28A; Bruker Advanced X-ray Solutions, Inc.: Madison, WI, 2001.
(17) *SADABS, Area Detector Absorption and other Corrections Software*, version 2.03; Bruker Advanced X-ray Solutions, Inc.: Madison, WI, 2000.
(18) Sheldrick, G. M. *SHELXTL*, version 6.10; Bruker Advanced X-ray Solutions, Inc.: Madison, WI, 2000.
(19) Lin, C.; Ren, T.; Valente, E. J.; Zubkowski, J. D.; Smith, E. T. *Chem. Lett.* **1997**, 753.

Table 1. Crystal Data and Structure Refinement Parameters for $Ru_2(O_2CMe)_3(DXyl^{2,6}F)Cl(THF)\cdot 0.5THF$ (**1a**·0.5THF), $Ru_2(O_2CMe)_3(DXyl^{2,6}F)Cl(HDXyl^{2,6}F)\cdot$toluene (**1b**·toluene), *trans*-$Ru_2(O_2CMe)_2(DXyl^{2,6}F)_2Cl(THF)$ (**2a**), *trans*-$Ru_2(O_2CMe)_2(DXyl^{2,6}F)_2Cl\cdot 2$toluene (**2b**·2toluene), $Ru_2(DAniF)_4Cl\cdot 0.5CH_2Cl_2$ (**5**·$0.5CH_2Cl_2$), [*trans*-$Ru_2(\mu\text{-}OMe)_2(\mu\text{-}O_2CMe)_2(HDAniF)_4]Cl_2\cdot 4$MeOH (**6**·4MeOH), and $Ru_2(DAniF)_4(H_2O)_{0.5}$ (**7**)

	1a·0.5THF	**1b**·toluene	**2a**	**2b**·2toluene	**5**·$0.5CH_2Cl_2$	**6**·4MeOH	**7**
chemical formula	$C_{29}H_{40}ClN_2O_{7.5}Ru_2$	$C_{47}H_{55}ClN_4O_6Ru_2$	$C_{42}H_{52}ClN_4O_5Ru_2$	$C_{52}H_{60}ClN_4O_4Ru_2$	$C_{60.5}H_{61}Cl_2N_8O_8Ru_2$	$C_{70}H_{92}Cl_2N_8O_{18}Ru_2$	$C_{60}H_{61}N_8O_{8.5}Ru_2$
fw	774.22	1009.54	930.47	1042.63	1301.21	1606.56	1232.31
cryst system	monoclinic	orthorhombic	monoclinic	triclinic	tetragonal	trigonal (hex. ax.)	triclinic
space group	*C*2/*c*	$P2_12_12_1$	$P2_1/n$	$P\bar{1}$	*P*4/*n*	R3*c*	$P\bar{1}$
a (Å)	26.367(2)	14.810(2)	11.3515(7)	10.5857(4)	13.1343(6)	25.9706(9)	10.343(3)
b (Å)	13.7031(8)	14.894(2)	24.207(1)	10.7264(4)	13.1343(6)	25.9706(9)	10.363(3)
c (Å)	18.740(1)	22.232(3)	15.984(1)	22.1132(7)	16.579(2)	62.120(3)	13.892(4)
α (deg)	90	90	90	85.808(1)	90	90	80.290(5)
β (deg)	107.790(1)	90	106.622(1)	76.785(1)	90	90	75.769(5)
γ (deg)	90	90	90	85.183(1)	90	120	81.557(5)
V (Å^3)	6447.1(7)	4904.0(1)	4208.7(4)	2432.0(2)	2860.0(3)	36285(3)	1414.0(7)
Z	8	4	4	2	2	18	1
D_{calc} (g/cm^3)	1.595	1.367	1.468	1.424	1.511	1.323	1.447
abs coeff (mm^{-1})	1.067	0.718	0.828	0.724	0.684	0.508	0.597
R1, wR2 [$I > 2\sigma(I)$]	0.0285, 0.0713	0.0557, 0.1366	0.0348, 0.0818	0.0371, 0.0987	0.0233, 0.0620	0.0596, 0.1640	0.0396, 0.1052
R1, wR2 (all data)	0.0343, 0.0758	0.0670, 0.1471	0.0452, 0.0880	0.0438, 0.1032	0.0276, 0.0660	0.0834, 0.1838	0.0457, 0.1121
GOF	1.089	1.119	1.029	1.020	1.068	1.103	1.103

Scheme 1. Reactions of $Ru_2(O_2CMe)_4Cl$ with $HDXyl^{2,6}F$[a]

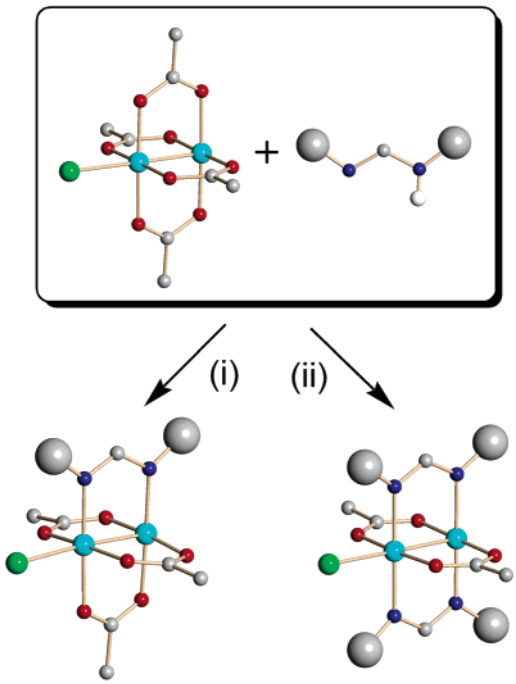

[a] Conditions: (i) toluene, 100 °C; (ii) molten $HDXyl^{2,6}F$, 160 °C.

is used, two acetate groups can be replaced and *trans*-$Ru_2(O_2CMe)_2(DXyl^{2,6}F)_2Cl$ (**2**) forms. The *transoid* arrangement of the bridging $DXyl^{2,6}F$ ligands was revealed by an X-ray structure determination (vide infra). The structural motif with two *transoid* formamidinate ligands has been previously observed in complexes of the Cr_2^{4+} and Mo_2^{4+} cores,[5,20,21] but there is only one Ru_2^{5+} complex with two acetate and two formamidinate groups at *transoid* positions. This was recently reported by Ren and obtained from the reaction of $Ru_2(O_2CMe)_4Cl$ with HDAni^{o}F after prolonged reflux in THF [HDAni^{o}F = *N*,*N*′-di(*o*-anisyl)formamidine].[22] However, that complex is not structurally analogous to **2** because one of the methyl groups of the anisyl groups of the bridging DAni^{o}F ligands is lost, and this allows the formation of a phenoxy group that coordinates axially to the Ru_2^{5+} unit, resulting in replacement of the Cl^- ion.

Further substitution of acetate groups in **2** was not possible, regardless of the experimental conditions employed (longer reaction time and higher temperature). This can be attributed to the large steric requirements of the 2,6-xylyl groups of the $DXyl^{2,6}F$ ligands, as shown by the space-filling model of **2** projected along the Cl−Ru−Ru axis (Figure S1). The bulkiness of the $DXyl^{2,6}F$ groups also supports the preference for the *transoid* arrangement of ligands around the Ru_2^{5+} core.

Reactions with HDAniF. The compounds isolated from reactions of $Ru_2(O_2CMe)_4Cl$ with *N*,*N*′-di(*p*-anisyl)formamidine under various conditions are summarized in Scheme 2. The first species isolated from such reactions, *cis*-$Ru_2(O_2CMe)_2(DAniF)_2Cl$, was originally prepared in 40% yield by reaction of $Ru_2(O_2CMe)_4Cl$ with HDAniF in a 1:2.5 ratio in refluxing THF or EtOH (ca. 70 °C). The product was isolated after a series of extractions that were followed by chromatographic purification.[11] We have now improved this synthesis by adding a small amount of LiCl and triethylamine to the reaction mixture. In this way, the crystalline product is isolated in 80% yield and can be used for further reactions without additional purification. In contrast to **2**, in which the formamidinate ligands adopt a *transoid* configuration, the *cisoid* arrangement forms exclusively when the less bulky DAniF ligand is used. The *cisoid* coordination of formamidinates has been observed in analogous compounds having M_2 cores, M = Mo and Rh,[23,24] and such species have been used in the construction of molecular squares, triangles and loops.[25]

(20) Cotton, F. A.; Daniels, L. M.; Murillo, C. A.; Schooler, P. *J. Chem. Soc., Dalton Trans.* **2000**, 2001.
(21) Wu, Y. Y.; Chen, J.-D.; Liou, L. S.; Wang, J. C. *Inorg. Chim. Acta* **2002**, *336*, 71.
(22) Ren, T.; DeSilva, V.; Zou, G. Lin, C.; Daniels, L. M.; Campana, C. F.; Alvarez, J. C. *Inorg. Chem. Commun.* **1999**, *2*, 301.
(23) Chisholm, M. H.; Cotton, F. A.; Daniels, L. M.; Folting, K.; Huffman, J. C.; Iyer, S. S.; Lin, C.; Macintosh, A. M.; Murillo, C. A. *J. Chem. Soc., Dalton Trans.* **1999**, 1387.
(24) Catalan, K. V.; Mindiola, D. J.; Ward, D. L.; Dunbar, K. R. *Inorg. Chem.* **1997**, *36*, 2458.
(25) Cotton, F. A.; Lin, C.; Murillo, C. A. *Proc. Natl. Acad. Sci. U.S.A.* **2002**, *99*, 4810.

Scheme 2. Reactions of $Ru_2(O_2CMe)_4Cl$ with HDAniF[a]

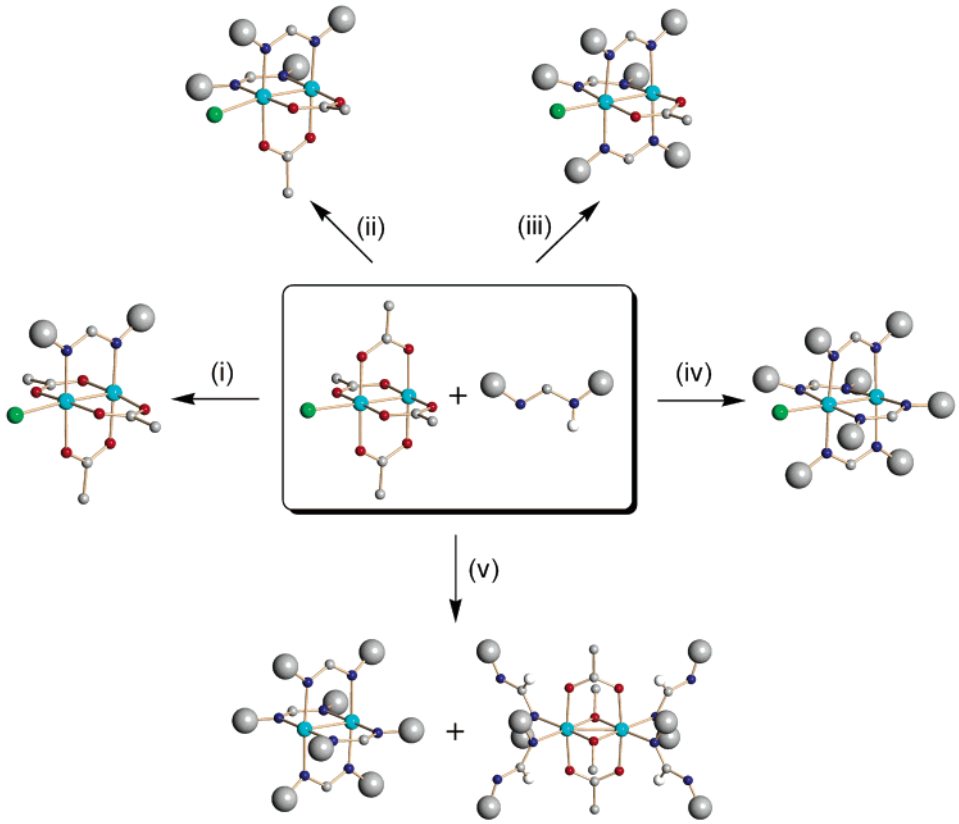

[a] Reagents and conditions: (i) $[Ru_2]^{5+}$/formamidine ratio R = 1:1.5, THF, 55 °C; (ii) R = 1:2, Et_3N/LiCl, THF, 70 °C; (iii) R = 1:2, Et_3N/LiCl, THF, 70 °C; (iv) R = 1:10, toluene, 110 °C; (v) R = 1:4, MeOH, 60 °C.

Early attempts to synthesize the mono- and tris-DAniF substituted Ru_2^{5+} complexes from the reactions of $Ru_2(O_2CMe)_4Cl$ with the corresponding stoichiometric amounts of HDAniF resulted in mixtures that had to be separated chromatographically and yields of only about 5%. For $Ru_2(O_2CMe)(DAniF)_3Cl$,[26] the selectivity and the yield were again greatly improved by adding LiCl and NEt_3 to the reaction mixture. However, this procedure is not as efficient for the preparation of $Ru_2(O_2CMe)_3(DAniF)Cl$, as substitution of a second acetate group proceeds rather rapidly, even at room temperature, giving a mixture of the unsubstituted starting material, which can be easily separated by filtration, and the mono- and the bis-DAniF substituted Ru_2^{5+} complexes, which required chromatographic separation. Optimization of the yield required close monitoring of the reaction mixture by thin-layer chromatography as a function of time and temperature. We noticed that the use of short reaction times, at room temperature, did not produce usable quantities of $Ru_2(O_2CMe)_3(DAniF)Cl$, and a large amount of the starting material $Ru_2(O_2CMe)_4Cl$ remained in the flask. Alternatively, long reaction times and high temperature favored the formation of the bis-DAniF substituted compound. However, it was found that this synthesis produced **3** in a consistent and usable yield of ca. 30% (which is similar to that for the $DXyl^{2,6}F$ analogue, **1**) when the reaction was carried out at ca. 40 °C for 12 h. Compounds **1** and **3** represent the first compounds having a Ru_2^{5+} core with one formamidinate and three acetate bridging ligands.

Solvent Influence. The type of solvent used in the reactions of $Ru_2(O_2CMe)_4Cl$ with HDAniF is of great importance, and THF appears to be the best solvent to control the selective formation of the variously DAniF substituted Ru_2^{5+} complexes. When the reaction of $Ru_2(O_2CMe)_4Cl$ with a 10-fold excess of HDAniF was carried out either in refluxing EtOH (ca. 75 °C) for 2−3 days or in refluxing toluene (ca. 110 °C) for 1−2 days, the fully substituted $Ru_2(DAniF)_4Cl$ (**5**) was the sole product, which was isolated in 80% yield as a purple microcrystalline solid. A similar result was obtained, although in lower yield, when HDAniF was used in smaller ratio, e.g., 1:6. Reactions of $Ru_2(O_2CMe)_4Cl$ with formamidines, such as HDPhF and HDTolF, also gave analogues of **5**.[27] It appears that the low solubility of the $Ru_2(DArF)_4Cl$ complexes in EtOH and toluene is an important driving force in shifting the equilibrium toward the fully substituted species.

Moreover, some solvents can promote additional reactions. In refluxing MeOH, two different compounds were isolated: the oxidized $Ru^{3+}Ru^{3+}$ edge-sharing bioctahedral

(26) The synthesis of $Ru_2(O_2CMe)(DAniF)_3Cl$ was reported earlier (see ref 12). Cyclic voltammetry measurements recorded in THF using $(Bu^n_4N)PF_6$ (V vs Ag/AgCl): $E_{1/2}(1) = +0.624$ V [$E_{ap}(1) = +0.680$ V and $E_{cp}(1) = +0.568$ V], $E_{ap}(2) = -0.253$ V, $E_{cp}(3) = -0.709$ V, $E_{ap}(4) = -1.485$ V, and $E_{cp}(4) = -1.607$ V.

(27) The compounds were identified as $Ru_2(DPhF)_4Cl$ and $Ru_2(DTolF)_4Cl$ by comparison of the unit cell parameters, which were the same (within the experimental error) as those reported. See: Bear, J. L.; Han, B.; Kadish, K. M. *Inorg. Chem.* **1996**, *35*, 3012 and ref 9, respectively.

complex [*trans*-$Ru_2(\mu\text{-}OMe)_2(\mu\text{-}O_2CMe)_2(HDAniF)_4]Cl_2$ (**6**) with a Ru−Ru single bond and the reduced Ru_2^{4+} complex $Ru_2(DAniF)_4$ (**7**). Few examples are known of disproportionation of a Ru_2^{5+} core[28] and even fewer examples in which the oxidized product has been isolated.[29] At present, it is not clear why methanol promotes this disproportionation process, which can be described with the general equation

$$2Ru_2^{5+} \rightarrow Ru_2^{4+} + Ru^{3+}Ru^{3+}$$

Compound **6** is the first edge-sharing bioctahedral diruthenium complex with bridging acetate and MeO groups in *transoid* positions to each other defining a symmetrical N_4O_2 coordination environment around the singly bonded Ru^{3+}-Ru^{3+} unit. It should be noted that disruption of the Ru−Ru bond in $Ru_2(O_2CMe)_4Cl$ upon reactions with *N*-donor ligands in MeOH and the formation of $Ru^{3+}Ru^{3+}$ edge-sharing bioctahedral complexes has been recognized in the past. For example, when $Ru_2(O_2CMe)_4Cl$ was reacted with 1-MeIm (1-MeIm = 1-methylimidazole) in MeOH, the complex $[Ru_2(\mu\text{-}OMe)(\mu\text{-}O_2CC_6H_4\text{-}p\text{-}OMe)_3(1\text{-}MeIm)_4](ClO_4)_2$, with only one bridging MeO group and a N_4O_2 coordination environment around a $Ru^{3+}Ru^{3+}$ unit, was obtained.[30] However, in that case, no other products were isolated or detected that would suggest a disproportionation process. The reduced product, $Ru_2(DAniF)_4$, is only the second crystallographically characterized Ru_2^{4+} tetraformamidinate complex, the first one being $Ru_2(DTolF)_4$.[8]

Crystal Structures. Complex **1** was crystallized from THF/hexanes as the THF adduct together with interstitial THF molecules, $Ru_2(O_2CMe)_3(DXyl^{2,6}F)Cl(THF)\cdot 0.5THF$ (**1a**·0.5THF). A drawing of a molecule of **1a** is shown in Figure 1, and selected bond distances and angles are listed in Table 2. The Ru(1)−Ru(2) bond distance of 2.3053(3) Å is between those observed in the chloro derivatives of Ru_2^{5+} tetracarboxylate and tetraformamidinate species, which are in the ranges of 2.27−2.30 and 2.34−2.39 Å, respectively. The average of the Ru−N distances is 2.030(3) Å. There are two different Ru−O distances: one for the acetate group trans to the $DXyl^{2,6}F$ ligand and another one for the two acetate groups cis to $DXyl^{2,6}F$. The former are slightly longer than the latter, with average distances of 2.060(2) Å and 2.039(4) Å, respectively, a difference that can be ascribed to a stronger trans influence of the $DXyl^{2,6}F$ ligand. The coordination environment of the Ru_2^{5+} unit is completed by two axial ligands, a Cl^- ion at a distance of 2.4629(7) Å and a THF molecule at a distance of 2.326(6) Å. The Cl^- ion is essentially aligned with the dimetal core with a Ru(2)−Ru(1)−Cl angle of 175.4(2)°, while the analogous angle

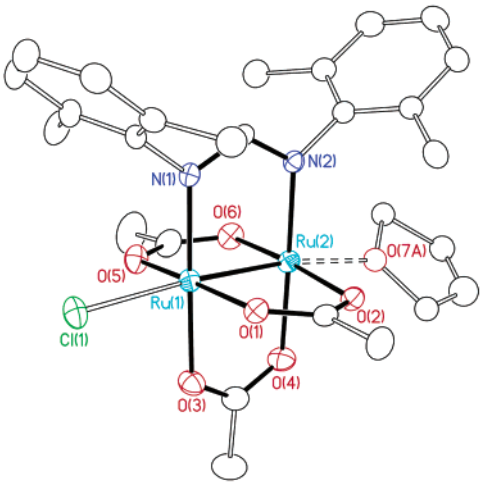

Figure 1. View of $Ru_2(O_2CMe)_3(DXyl^{2,6}F)$ Cl(THF) in **1a**·0.5THF with the atoms represented by thermal ellipsoids at the 35% probability level. Hydrogen atoms are omitted for clarity.

Table 2. Selected Bond Distances (Å) and Angles (deg) for $Ru_2(O_2CMe)_3(DXyl^{2,6}F)Cl(THF)\cdot 0.5THF$ (**1a**·0.5THF)

Bond Distances			
Ru(1)−Ru(2)	2.3053(3)	Ru(2)−O(2)	2.025(2)
Ru(1)−N(1)	2.036(2)	Ru(2)−O(4)	2.060(2)
Ru(2)−N(2)	2.023(2)	Ru(2)−O(6)	2.026(2)
Ru(1)−O(1)	2.059(2)	Ru(1)−Cl(1)	2.4629(7)
Ru(1)−O(3)	2.060(2)	Ru(2)···O(7A)	2.326(6)
Ru(1)−O(5)	2.047(2)		

Bond Angles			
N(1)−Ru(1)−O(1)	91.47(7)	N(2)−Ru(2)−O(6)	92.00(8)
N(1)−Ru(1)−O(3)	178.41(8)	N(1)−Ru(1)−Ru(2)	90.13(5)
N(2)−Ru(2)−O(4)	178.77(8)	O(1)−Ru(1)−Ru(2)	87.99(5)
O(1)−Ru(1)−O(3)	88.87(7)	O(1)−Ru(1)−Cl(1)	92.16(5)
O(5)−Ru(1)−O(1)	173.87(7)	Ru(2)−Ru(1)−Cl(1)	175.40(2)
O(2)−Ru(2)−O(6)	174.68(7)	Ru(1)−Ru(2)···O(7A)	170.4(2)

with the O atom of THF molecule is slightly more off line with a Ru(1)−Ru(2)···O(7A) angle of 170.4(2)°. This is probably due to the existence of nonbonding repulsions with the sterically demanding 2,6-xylyl groups of the bridging formamidinate ligand.

Because an excess of formamidine was used in the reaction, the solid isolated from the reaction mixture always contained a small amount of unreacted $HDXyl^{2,6}F$. When this solid was dissolved in a coordinating solvent, such as THF, the excess formamidine remained in solution during the crystallization process. However, in noncoordinating solvents, such as toluene, another crystalline form, $Ru_2(O_2CMe)_3(DXyl^{2,6}F)Cl(HDXyl^{2,6}F)$ (**1b**), in which an $HDXyl^{2,6}F$ molecule occupies one axial position was obtained. Its structure is shown in Figure S2. In general, there are no significant differences between the structures **1a** and **1b**. However, the Ru(1)−Ru(2) bond distance in **1b** of 2.3326(8) Å is slightly longer than the corresponding distance in **1a** [2.3053(3) Å]. This can be attributed to the better donor character (greater basicity) of the $HDXyl^{2,6}F$ molecule relative to THF. The averages of the Ru−N distances and Ru−O distances are similar to those in **1a**. One nitrogen atom of the axial $HDXyl^{2,6}F$ molecule is at a distance of 2.388(5) Å from the Ru_2^{5+} core, and the Ru(1)−Ru(2)−N(3) angle is 168.8(2)°.

(28) See for example: (a) Cotton, F. A.; Miskowski, V. M.; Zhong, B. *J. Am. Chem. Soc.* **1989**, *111*, 6177. (b) Cotton, F. A.; Labella, L.; Shang, M. *Inorg. Chim. Acta* **1992**, *197*, 149. (c) Barral, M. C.; Jiménez-Aparicio, R.; Priego, J. L.; Royer, E. C.; Urbanos, F. A.; Amador, U. *Inorg. Chim. Acta* **1998**, *279*, 30.

(29) See, for example:(a) Barral M. C.; Jiménez-Aparicio R.; Kramolowsky R.; Wagner I. *Polyhedron*, **1993**, *12*, 903. (b) Barral, M. C.; Jiménez-Aparicio, R.; Royer, E. C.; Saucedo, J. M.; Urbanos, F. A.; Gutiérrez-Puebla, E.; Ruiz-Valero, C. *J. Chem. Soc., Dalton Trans.* **1991**, 1609.

(30) Sudha, C.; Mandal, S. K.; Chakravarty, A. R. *Inorg. Chem.* **1994**, *33*, 4878.

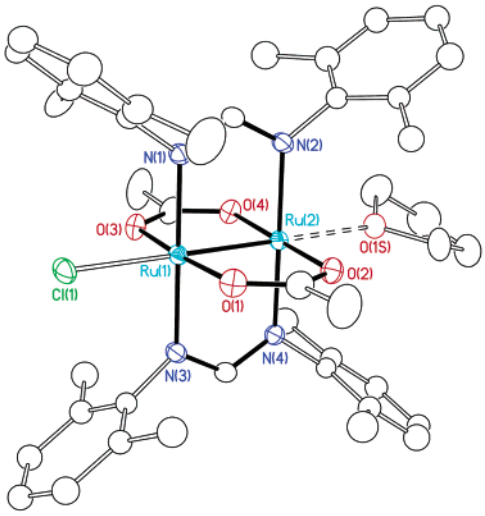

Figure 2. View of *trans*-$Ru_2(O_2CMe)_2(DXyl^{2,6}F)Cl(THF)$ (**2a**) with the atoms represented by thermal ellipsoids at the 35% probability level. H atoms are omitted for clarity.

Table 3. Selected Bond Distances (Å) and Angles (deg) for *trans*-$Ru_2(O_2CMe)_2(DXyl^{2,6}F)_2Cl(THF)$ (**2a**)

Bond Distances			
Ru(1)−Ru(2)	2.3259(3)	Ru(2)−N(4)	2.069(2)
Ru(1)−N(1)	2.071(2)	Ru(2)−O(2)	2.018(2)
Ru(1)−N(3)	2.074(2)	Ru(2)−O(4)	2.036(2)
Ru(1)−O(1)	2.049(2)	Ru(1)−Cl(1)	2.4415(7)
Ru(1)−O(3)	2.057(2)	Ru(1)−O(1S)	2.407(2)
Ru(2)−N(2)	2.072(2)		

Bond Angles			
N(1)−Ru(1)−N(3)	179.5(1)	N(2)−Ru(2)−O(4)	89.09(9)
N(1)−Ru(1)−O(1)	89.04(9)	N(1)−Ru(1)−Ru(2)	90.18(6)
N(3)−Ru(1)−O(1)	90.53(9)	O(1)−Ru(1)−Ru(2)	87.21(6)
O(1)−Ru(1)−O(3)	174.79(8)	O(1)−Ru(1)−Cl(1)	91.23(6)
N(2)−Ru(2)−N(4)	179.04(9)	Ru(2)−Ru(1)−Cl(1)	179.55(2)
N(2)−Ru(2)−O(2)	90.39(9)	Ru(1)−Ru(2)−O(1S)	178.14(6)

Similarly to **1**, *trans*-$Ru_2(O_2CMe)_2(DXyl^{2,6}F)_2Cl$ was also crystallized in two different forms depending on the solvent used for crystallization. In THF, *trans*-$Ru_2(O_2CMe)_2(DXyl^{2,6}F)_2Cl(THF)$, **2a**, formed. However, in a noncoordinating solvent, such as toluene, $Ru_2(O_2CMe)_2(DXyl^{2,6}F)_2Cl$ (**2b**) together with two interstitial molecules of toluene was crystallized. Unlike **1b**, which has an axial formamidine molecule, **2b** contains no such molecule. It appears that the combined effect of the substituents in two formamidinate anions makes the coordination environment of the Ru_2^{5+} unit so crowded that the axial positions are inaccessible to the bulky $HDXyl^{2,6}F$ molecules. Drawings of **2a** and **2b** are shown in Figures 2 and S3, respectively, and selected bond distances and angles for **2a** are presented in Table 3. The Ru(1)−Ru(2) bond length of 2.3259(3) Å in **2a** is only slightly longer than the corresponding distance in **1a**, and it is in the range of the distances observed in the Ru_2^{5+} tetracarboxylate and tetraformamidinate complexes. The average of the Ru−N distances is 2.072(4) Å, while the average of the Ru−O distances of 2.040(4) Å is slightly shorter. As in **1a**, in **2a**, there are two axially coordinated ligands, a Cl^- ion and a THF molecule. The anion is at a distance of 2.4415(7) Å from the Ru_2^{5+} unit (slightly shorter than in **1a**), forming an almost linear chain with the two Ru atoms with a Ru(2)−Ru(1)−Cl(1) angle of 179.55(2)°. The latter is at a distance of 2.407(2) Å, which is longer than the Ru···O distance in **1a** because of the steric repulsion of the THF molecule with the 2,6-xylyl groups of two formamidinate ligands rather than one found in **1a**, and it forms an almost linear Ru(1)−Ru(2)···O(5) angle of 178.14(6)°. In **2b**, the Ru(1)−Ru(2) bond length of 2.3157(3) Å is slightly shorter than the 2.3259(3) Å length found in **2a**. This can be attributed to the presence of an additional axially coordinated THF molecule in **2a** that lengthens the Ru−Ru bond. Except for this, there are no other significant differences in the structural characteristics between **2a** and **2b**.

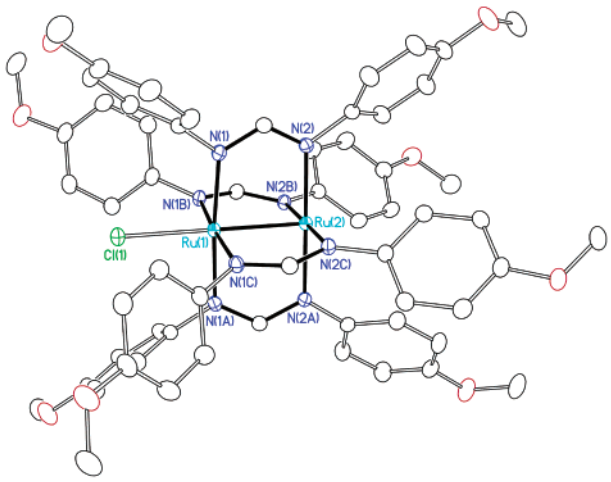

Figure 3. View of the molecule $Ru_2(DAniF)_4Cl$ in **5**·$0.5CH_2Cl_2$ with the atoms represented by thermal ellipsoids at the 35% probability level. H atoms are omitted for clarity. Selected bond distances (Å) are as follows: Ru(1)−Ru(2) 2.396(1), Ru(1)−N(1) 2.074(2), Ru(2)−N(2) 2.048(1), and Ru(1)−Cl(1) 2.438(1).

The fully substituted compound **5** was crystallized from CH_2Cl_2/hexanes as $Ru_2(DAniF)_4Cl$ together with one-half of an interstitial CH_2Cl_2 molecule. The molecule lies on a crystallographic C_4 axis, which coincides with the Ru(2)−Ru(1)−Cl(1) unit. Its structure is shown in Figure 3. The Ru(1)−Ru(2) bond distance of 2.3960(4) Å is only slightly longer than that of 2.370(2) Å in $Ru_2(DTolF)_4Cl$, the first structurally characterized Ru_2^{5+} tetraformamidinate complex.[9] In contrast to **1a** and **2a**, the bridging ligands are not in a fully eclipsed conformation, with a torsion angle of 7.4(4)° of the DAniF ligands about the Ru−Ru bond, which results in two different Ru−N distances of 2.074(2) Å at Ru(1) and 2.048(1) Å at Ru(2). The axially coordinated Cl^- ion is at a distance of 2.4380(8) Å from Ru(1), forming a rigorously linear chain with the Ru_2^{5+} unit. Interstitial CH_2Cl_2 molecules are found between the Ru_2^{5+} units.

The crystal structure of **6** consists of the cation [*trans*-$Ru_2(\mu\text{-}OMe)_2(\mu\text{-}O_2CMe)_2(HDAniF)_4]^{2+}$, two Cl^- ions, and four interstitial MeOH molecules. The cation lies on a crystallographic inversion center that coincides with the midpoint of the Ru(1)−Ru(1A) bond. As shown in Figure S4, two Ru^{3+} atoms are bridged by two trans acetate and two trans MeO ligands; four terminal neutral HDAniF ligands complete the coordination sphere of the metal centers defining the edge-sharing bioctahedron. The Ru(1)−Ru(1A) distance of 2.5009(7) Å is one of the shortest distances

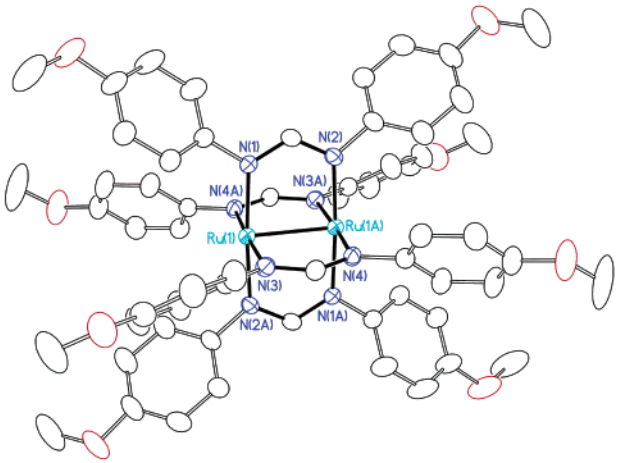

Figure 4. View of the $Ru_2(DAniF)_4$ molecule in **7** with the atoms represented by thermal ellipsoids at the 35% probability level. The axially coordinated H_2O molecules and H atoms are omitted for clarity. Selected bond distances (Å) are as follows: Ru(1)−Ru(1A) 2.454(1), Ru(1)−N(1) 2.051(3), Ru(2)−N(3) 2.052(3), Ru(1)−N(2A) 2.040(3), and Ru(1)−N(4A) 2.047(3).

Table 4. Selected Bond Distances (Å) and Angles (deg) for $Ru_2(DAniF)_4(H_2O)_{0.5}$ (**7**)

Bond Distances			
Ru(1)−Ru(1A)	2.4529(7)	Ru(1)−N(2A)	2.039(3)
Ru(1)−N(1)	2.051(3)	Ru(1)−N(4A)	2.046(3)
Ru(1)−N(3)	2.053(3)		
Bond Angles			
N(1)−Ru(1)−N(3)	89.9(1)	N(3)−Ru(1)−N(4A)	176.3(1)
N(1)−Ru(1)−N(2A)	176.4(1)	Ru(1A)−Ru(1)−N(1)	88.42(8)
N(3)−Ru(1)−N(2A)	88.9(1)	Ru(1A)−Ru(1)−N(3)	89.99(8)

observed in edge-sharing bioctahedral complexes of the Ru^{3+}-Ru^{3+} unit.[31] The close proximity of the two Ru centers is probably caused by the small bite angle of the bridging acetate and MeO groups, which results in the enhancement of the d orbital overlap of the Ru atoms. The oxygen atoms of the bridging methoxy groups are at distances of 2.022(3) Å from the Ru atoms, forming acute Ru−O−Ru angles of 76.4(1)°, while the Ru−O distances for the $MeCO_2$ ligands are slightly longer at 2.083(3) Å. The average Ru−N distance to the terminal HDAniF ligands is 2.072(4) Å.

A view of compound **7**, with the reduced Ru_2^{4+} core, is shown in Figure 4. The complex lies on a crystallographic inversion center that coincides with the midpoint of the Ru(1)−Ru(1A) bond. The Ru(1)−Ru(1A) bond length of 2.4529(7) Å (Table 4) is very close to the corresponding distance of 2.474(1) Å in the only other known Ru_2^{4+} tetraformamidinate compound, $Ru_2(DTolF)_4$.[8] The average of the Ru−N distances is 2.047(6) Å. The bridging formamidinate ligands are nearly eclipsed (torsion angle of ca. 1°), in contrast to $Ru_2(DTolF)_4$ in which the torsion angle is ca. 9°.

Electrochemistry. The electrochemistry of the DXylF complexes **1a** and **2a** and the $Ru_2(O_2CMe)_{4-n}(DAniF)_nCl$ species was studied in THF solutions. Several redox processes are involved, and with small but important variations, the CVs (Figures S5 and S6) resemble those reported earlier

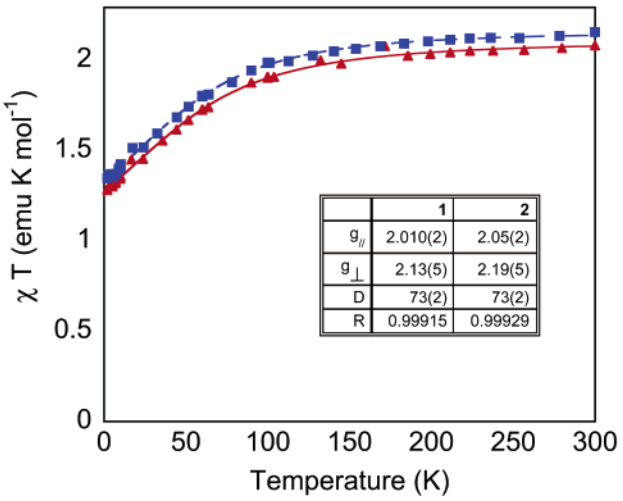

Figure 5. Magnetic susceptibility data for **1** (red triangles) and **2** (blue squares). Solid lines are the least-squares fits based on equations from ref 35.

for other $Ru_2(formamidinate)_4^+$ species[19] and for some of the carboxylate analogues.[32,33] Compounds **1** and **2** exhibit similar behaviors: each displays one metal-centered oxidation process, which corresponds to the redox couple Ru_2^{5+}/Ru_2^{6+}, and a metal-centered reduction process, attributed to the redox couple Ru_2^{5+}/Ru_2^{4+}. The oxidation process is more reversible for **2** than for **1**. It appears that the presence of a second basic $DXyl^{2,6}F$ ligand allows the oxidation process to take place at a more accessible potential [$E_{1/2}(1) = +0.933$ V vs $E_{ap}(1) = +1.295$ V for **2** and **1**, respectively].

For the DAniF complexes $Ru_2(O_2CMe)_{4-n}(DAniF)_nCl$, there are reversible processes at $E_{1/2} = +0.817$, $+0.624$, and $+0.431$V for the complexes with $n = 2-4$, respectively, that correspond to the redox couple Ru_2^{5+}/Ru_2^{6+}. The oxidation reaction $Ru_2^{5+} \rightarrow Ru_2^{6+} + e^-$ becomes easier as the number of DAniF ligands increases, as expected because of the higher basicity of DAniF ligands relative to the acetate groups. Irreversible cathodic processes at $E_{cp} = -0.668$, -0.709, and -0.754 V, for $n = 2-4$, respectively, can be assigned to the reductions $Ru_2^{5+} + e^- \rightarrow Ru_2^{4+}$. These complexes also exhibit anodic waves at $E_{ap} = -0.297$, -0.253, and -0.155 V for $n = 2-4$, respectively, that can be attributed to the couples $[Ru_2(O_2CMe)_{4-n}(DAniF)_n(THF)_2]^+$/$Ru_2(O_2CMe)_{4-n}(DAniF)_n(THF)_2$. This assignment is supported by the fact that addition of a large excess of Cl^- ions during the electrochemical experiment causes these signals to disappear. The cathodic peaks for these couples were not observed, suggesting that dissociation of Cl^- ion is not favorable for these Ru_2^{5+} complexes.

Magnetism and Electronic Structures. All Ru_2^{5+} compounds are paramagnetic in the temperature range of 3−300 K. Compounds **1a** and **2b** exhibit similar behavior. A plot of $\chi_M T$ values per Ru_2^{5+} unit versus temperature for **1a** is shown in Figure 5. For both complexes, the room-temperature $\chi_M T$ value per Ru_2^{5+} unit is ca. 1.75 emu·K/mol, and the magnetism gradually decreases upon cooling. At 3 K,

(31) See, for example: Miyasaka, H.; Chang, H.-C.; Mochizuki, K.; Kitagawa, S. *Inorg. Chem.* **2001**, *40*, 3544.

(32) Cotton, F. A.; Pedersen, E. *Inorg. Chem.* **1975**, *14*, 388.

(33) Malinski, T.; Chong, D.; Feldmann, F. N.; Bear, J. L.; Kadish, K. M. *Inorg. Chem.* **1983**, *22*, 3225.

this value is ca. 1.05 emu·K/mol for both **1a** and **2b**. A decrease of the $\chi_M T$ values is common for diruthenium compounds and has been attributed to contributions of zero-field splitting (ZFS).[34] Simulations performed using the Van Vleck equation for an axially symmetric system with $S = {}^3/_2$ and a ZFS contribution (D)[35] provide the best-fitting parameters of $g_{\|} = 2.01(2)$, $g_{\perp} = 2.13(5)$, $D = 73(2)$ cm^{-1} ($R = 0.99915$) for **1a** and $g_{\|} = 2.05(2)$, $g_{\perp} = 2.19(5)$, and $D = 73(2)$ cm^{-1} ($R = 0.99929$) for **2**. These values are in good agreement with those reported for Ru_2^{5+} paddlewheel compounds[34] and are consistent with **1a** and **2b** having the usual $\sigma^2\pi^4\delta^2(\pi^*\delta^*)^3$ ground-state electronic configuration. The DAniF compounds $Ru_2(O_2CMe)_{4-n}(DAniF)_nCl$ with $n = 2$ and 3 also have three unpaired electrons and a $\sigma^2\pi^4\delta^2(\pi^*\delta^*)^3$ ground-state electronic configuration, and they undergo a significant zero-field splitting.[11,12,34]

Complexes **6** and **7** are diamagnetic, on the basis of the sharp signals and their positions in the ^{1}H NMR spectra. The Ru_2^{6+} compound **6** with an edge-sharing bioctahedral structure has a long Ru−Ru bond distance of 2.501(1) Å, which is in accordance with a singly bonded diruthenium unit and a $\sigma^2\pi^2\delta^2\delta^{*2}\pi^{*2}$ electronic configuration (the d_{xy} orbitals of the two Ru atoms are used to form bonds with the bridging MeO groups, leaving the d_{xz} orbitals to form the π and π^* molecular orbitals). The paddlewheel complex **7** has a Ru_2^{4+} unit with a $\sigma^2\pi^4\delta^2\pi^{*4}$ ground-state electronic configuration. The diamagnetism of this complex can be attributed to the rising of the δ^* molecular orbital above the π^* molecular orbitals of the Ru_2^{4+} core because of the increased interaction with the orbitals of the basic *N*,*N*′-donor bridging ligands. Analogous complexes of the Ru_2^{4+} core with *N*,*N*′-donor bridging ligands, i.e., $Ru_2(DTolF)_4$[8] and $Ru_2(DTolTA)_4$,[36] have shown similar behavior.

Concluding Remarks

The entire set of $Ru_2(O_2CMe)_{4-n}(DArF)_nCl$ compounds with $n = 1-4$ and Ar = an aryl group (2,6-xylyl or *p*-anisyl) have now been prepared. These compounds can serve as precursors to a variety of corner pieces for the syntheses of higher-order, paramagnetic architectures by utilizing the significantly greater lability of the acetate groups compared to the formamidinate groups, which allows for selective substitution of the acetate groups. The complexes $Ru_2(O_2CMe)_2(DArF)_2Cl$ have been made in the cis and trans forms by controlling the size of the substituents of the formamidinate ligands. The bulky DXylF anion favors the trans form, which has the potential of producing ladder-type architectures with suitable linkers, whereas the less bulky DAniF ligands give the cis form, which is capable of producing squares, loops, or triangles with suitably chosen linkers. The complexes $Ru_2(O_2CMe)_3(DArF)Cl$ and $Ru_2(O_2CMe)(DArF)_3Cl$[12,37] have also been synthesized. Yields for all complexes are in the usable range of 30−80%.

Current work in our laboratory involves the use of these precursors in reactions with appropriate linkers in order to synthesize polymeric architectures, such as one-dimensional ladders, **VIII**, and two-dimensional grids, **IX**.

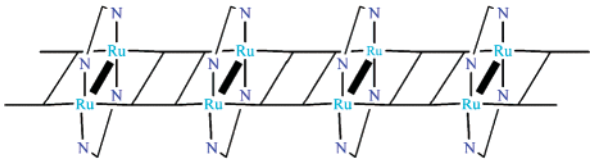

VIII

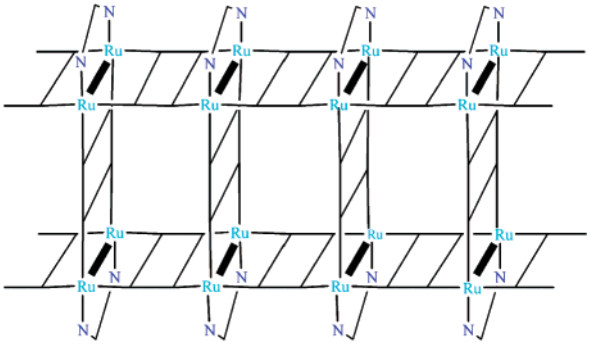

IX

In addition, by utilizing the axial coordination the synthesis of three-dimensional architectures is expected. Such assemblies might exhibit gas absorption properties, as their cavities might be capable of accommodating guest molecules (e.g., noble gases).[38,39] Furthermore, given the paramagnetic nature of the Ru_2^{5+} units, such supramolecular assemblies might have the potential to open the way to the construction of novel multidimensional materials that could exhibit magnetic[40] and/or conductivity properties.[41]

Acknowledgment. We thank the National Science Foundation and the Welch Foundation for financial support. We

(34) See, for example: (a) Telser, J.; Drago, R. S. *Inorg. Chem.* **1984**, *23*, 3114. (b) Telser, J.; Miskowski, V. M.; Drago, R. S.; Wong, N. M. *Inorg. Chem.* **1985**, *24*, 4765. (c) Cukiernik, F. D.; Luneau, D.; Marchon, J.-C.; Maldivi, P. *Inorg. Chem.* **1998**, *37*, 3698 and references therein. (d) Miskowski, V. M.; Hopkins, M. D.; Winkler, J. R.; Gray, H. B. In *Inorganic Electronic Structure and Spectroscopy, Volume II: Applications and Case Studies*; Solomon, E. I., Lever, A. B. P., Eds.; John Wiley & Sons: New York, 1999; pp 343−402.

(35) The equations utilized are

$$\chi_{\|} = \frac{Ng_{\|}^2\beta^2}{kT} \cdot \frac{1 + 9\exp(-2D/kT)}{4[1 + \exp(-2D/kT)]}$$

$$\chi_{\perp} = \frac{Ng_{\perp}^2\beta^2}{kT} \cdot \frac{4 + (3kT/D)[1 - \exp(-2D/kT)]}{4[1 + \exp(-D/kT)]}$$

where χ is the molar magnetic susceptibility, k is the Boltzmann constant, N is Avogadro's number, and D is the ZFS parameter; the average of χ is given by

$$\chi = \frac{\chi_{\|} + 2\chi_{\perp}}{3}$$

These equations have been used successfully in previous studies from this and other groups for [Ru_2] systems having $S = {}^3/_2$ ground states, large anisotropies, and large ZFS. See, for example, refs 11, 12, 24, and 34.

(36) Cotton, F. A.; Matusz, M. *J. Am. Chem. Soc.* **1988**, *110*, 5761.

(37) Barral, M. C.; Herrero, S.; Jiménez-Aparicio, R.; Torres, M. R.; Urbanos, F. A. *Inorg. Chem. Commun.* **2004**, *7*, 42.

(38) Takamizawa, S.; Mori, W.; Furihata, M.; Takeda, S.; Yamaguchi, K. *Inorg. Chim. Acta* **1998**, *283*, 268.

(39) Takamizawa, S.; Ohmura, T.; Yamaguchi, K.; Mori, W. *Mol. Cryst. Liq. Cryst.* **2000**, *342*, 199.

(40) Liao, Y.; Shum, W. W.; Miller, J. S. *J. Am. Chem. Soc.* **2002**, *124*, 9336.

(41) Akutagawa, T.; Hasegawa, T.; Nakamura, T.; Inabe, T. *J. Am. Chem. Soc.* **2002**, *124*, 8903.

also thank Prof. K. R. Dunbar and Dr. A. Prosvirin for helpful discussions of the magnetic data.

Supporting Information Available: Crystallographic data in CIF format for compounds **1a**·0.5THF, **1b**·toluene, **2a**, **2b**·2toluene, **5**·0.5CH_2Cl_2, **6**·4MeOH, and **7**. Space-filling model of **2a** (Figure S1); structures of **1b** (Figure S2), **2b** (Figure S3), and **6** (Figure S4); and cyclic voltammograms of **1a** and **2a** (Figure S5) and of **4**, **5**, and $Ru_2(O_2CMe)(DAniF)_3Cl$ (Figure S6). Selected bond distances and angles for **1b**·toluene, **2b**·2toluene, **5**·0.5CH_2Cl_2, and **6**·4MeOH in Tables S1−S4, respectively. This material is available free of charge via the Internet at http://pubs.acs.org.

IC049108W